AGRICULTURAL CROP TYPE MAPPING USING OBJECT-BASED IMAGE ANALYSIS WITH ADVANCED ENSEMBLE LEARNING ALGORITHMS

Taskin Kavzoglu (1), Ismail Colkesen (1), Hasan Tonbul (1)

[1]Gebze Technical University, Geomatics Engineering Department, 41400, Gebze-Kocaeli, Turkey
Email: kavzoglu@gtu.edu.tr; icolkesen@gtu.edu.tr; htonbul@gtu.edu.tr

KEY WORDS: Agriculture, Ensemble Learning, OBIA, Segmentation, WorldView-2

ABSTRACT: Parallel to the rapid technological advances, up-to-date remote sensing platforms and sensors have made it possible to observe the Earth's surface features at a higher spatial and spectral resolution. The WorldView-2 (WV-2) imagery has been effectively used for the detailed mapping of agricultural crop-type types in many studies. The selected area for this study covers approximately 17 km^2 of various agricultural land and forest areas. Hazelnut and corn products, which are spectrally similar crop types, are the most dominant and economically valuable agricultural products for this particular region. Therefore, accurate determination of these agricultural products and mapping of their spatial locations play important role for yield estimation. The primary objective of this paper is to map cultivated areas by classifying a WV-2 imagery using conventional classifiers and advanced ensemble learning algorithms. In addition, several spectral indices were used as an ancillary dataset to identify and differentiate cultivated areas and forest species from each other. Within this context, object-based image analysis (OBIA) with multi-resolution segmentation was performed to produce image objects. Then, a total of 22 image object subsets were determined for the segmented image objects. Four classification algorithms, namely Random Forest (RF), Canonical Correlation Forest (CCF), Decision Tree (DT), and k-nearest neighbor (k-NN) classifiers were applied to produce the thematic map of the study area. Result of the study showed that the CCF classifier reached the highest overall accuracy of 94% with dataset having 22 object subsets. The improvement in classification performance reached to 7% in terms of overall classification accuracy. Moreover, the results noticeably indicated that ensemble methods (i.e., RF and CCF) outperformed the DT and k-NN classifiers in terms of applied accuracy measures. The results were confirmed by the McNemar's statistical test. Moreover, feature importance results of the RF algorithm showed that the most important vegetation indices were Chlorophyll RedEdge, green leaf, and NDVI-2 indices, respectively.

1. INTRODUCTION

Mapping cultivated areas using remote sensing technologies provides significant advantages in terms of cost and time required for traditional mapping methods. Satellite observations enable reliable and up-to-date data about the Earth's surface. The use of optical images has significantly contributed to determining crop products (Inglada et al., 2015; Mokhtari et al., 2019). There has been an increasing amount of literature on the mapping of agricultural lands using satellite imagery with different spectral resolution (Immitzer et al., 2012; Belgiu and Csillik, 2018; Sonobe et al., 2018).

The Worldview-2 (WV-2), the first commercial satellite having 2m spatial resolution with 8 multispectral bands, provides a great opportunity for cropland mapping thanks to its high spatial resolution and high revisiting time. It also provides an excessive contribution for monitoring agricultural fields due to its spectral bands covering the visible and NIR wavelength regions.

Spectral indices, combinations of spectral measurements at different wavelengths, have been widely used as an ancillary dataset for accurate determination of crop product types (Ghebreamlak et al., 2018; Sonobe et al., 2018). There is a wide range of spectral indices in the literature to distinguish and identify vegetation and agricultural product types. However, it is often not possible to use a large number of spectral indices together in the studies to be conducted. Furthermore, using more features than the optimum number may result in a decrease in accuracy achieved by the classifier, which is called ''curse of dimensionality' (Hughes, 1968). In general, data distributions in high-dimensional feature space have been found to cover a subspace of low dimensionality (Kavzoglu and Mather, 2002). Therefore, selecting features, which contributes to the highest separability between landscape features are essential for highest classification accuracy (Kavzoglu et al., 2018).

Classification algorithms are also very important in determining the classification accuracies of cropland maps (Sonobe et al., 2018). In particular, the use of non-parametric classifiers instead of parametric classifiers has been found to give higher accuracy in agricultural product mapping (Kavzoglu et al., 2018; Kenduiywo et al., 2018; Numbisi et al., 2019). In addition, in recent years, ensemble learning algorithms have been successfully applied to

many remote sensing studies mainly focused on agricultural activities due to their robustness (Colkesen and Kavzoglu, 2017; Kenduiywo et al., 2018; Colkesen and Kavzoglu, 2019).

The main idea of this research is to determine the potential use of WV-2 data for crop type mapping and the assessment of classification performances of Random Forest (RF), Canonical Forest (CCF), Decision Tree (DT), and k-nearest neighbor (k-NN) classifiers.

2. STUDY AREA AND DATASET

In this study, a radiometrically corrected, geo-referenced, orthorectified WV-2 multispectral high-resolution dataset was used. The multispectral bands were pan-sharpened using the Gram-Schmidt algorithm to improve the spatial resolution of the image from 2 to 0.5 m and the resulting image is in the size of 8611x7825 pixels. The test site chosen for the study is the Ferizli district of Sakarya province located in the northwest of Turkey (Figure 1). The study area covers approximately 17 km2 agricultural region. The main crop production in the region is concentrated on corn and hazelnuts. Depending on the landscape structure of the region, eleven land use/cover (LULC) categories, namely, water, agriculture, corn, hazelnut, road, soil, building, concrete, barren, shadow and forest were determined.

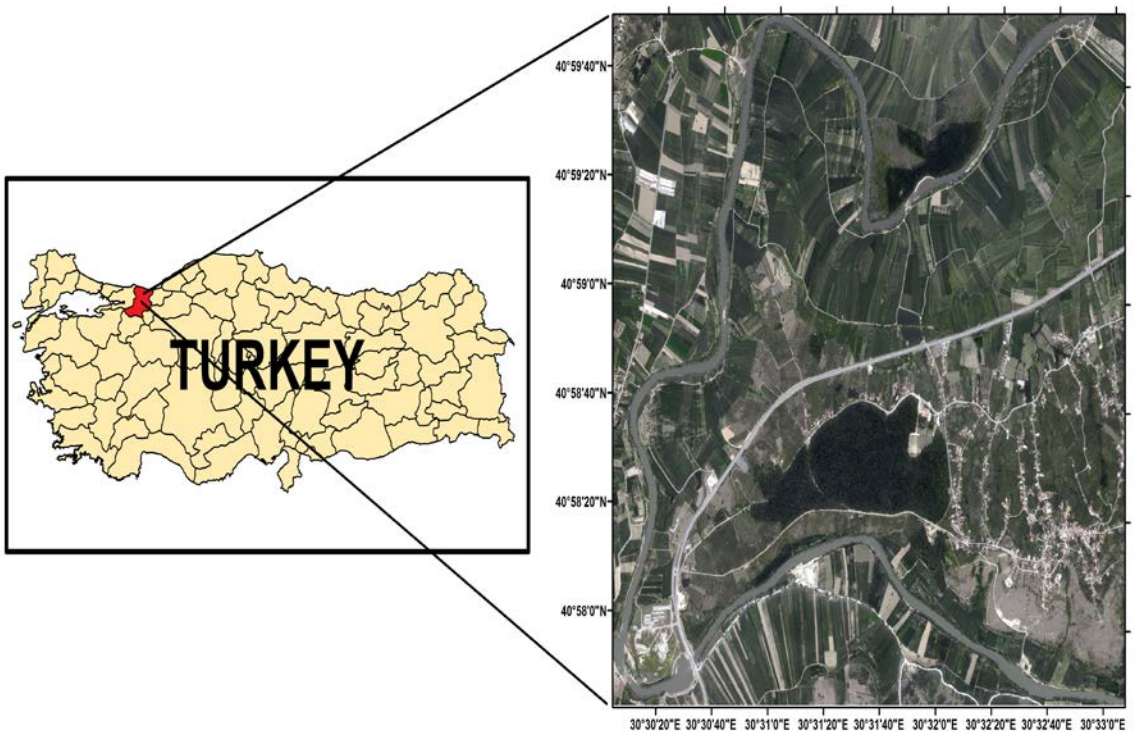

Figure 1. The location of the study site.

3. METHODOLOGY

In this study, a very high-resolution WV-2 imagery was classified using object-based image analysis (OBIA) with k-NN, DT, RF and CCF algorithms to produce detailed agricultural crop type map of the study area. In order to meet this purpose, the key processing steps of OBIA including image segmentation, classification of segmented objects and accuracy assessment were conducted, respectively.

3.1. Image segmentation

Image segmentation, which based on the creation of image objects, is the first and most vital process of OBIA. There are many segmentation algorithm and methods in the literature, which can be separated four main categories as thresholding, region-based, histogram image feature space clustering and edge-based segmentation (Cheng et al. 2001). Multi-resolution segmentation (Baatz and Schäpe, 2000) is one of the most popular and commonly used segmentation algorithms (Kavzoglu et al., 2016; 2017; Kavzoglu and Tonbul, 2018). It contains three parameters namely, scale, shape, compactness.

3.2. Classification algorithms

In order to classify segmented image segments with respect to their features, four classification algorithms including k-NN classifier, DT classifier and two advanced ensemble learning algorithms namely, RF and CCF were utilized. k-NN, known as a standard classification algorithm, has been widely used to solve many classification and regression problems in the literature (Liu et al., 2012; Mui et al., 2015). This method verifies the class label for the unknown sample based on its contiguous neighbor. In this method, it is assumed that the distribution in the set of points constituting the class control data is in the normal distribution.

DT algorithm uses a multi-purpose or sequential approach to perform the classification process. This technique does not involve any statistical assumption, so it is considered a nonparametric classification approach. The basic structure of a DT consists of three basic parts called node, branch and leaf. In this tree structure, each attribute or feature is represented by a node. Thus, a set of rules is defined to implement the classification process.

In order to apply above mentioned classic classification algorithms, two ensemble-based learning algorithms (i.e. RF and CCF) were also considered in this study. The RF algorithm, introduced by Breiman (2001) as a decision tree-based ensemble learning framework, has been widely used in the classification of remotely sensed imagery due to its success for discrimination of spectrally similar pixels belonging to different LULC classes (Kavzoglu and Colkesen, 2013; Colkesen and Kavzoglu, 2017). The main idea behind the algorithm is to construct multiple DT classifier using the different training datasets formed by applying bootstrap aggregation (i.e. bagging) and to estimate the class label of an unknown sample by combining their predictions. In order to improve the prediction accuracy of the RF, the CCF ensemble learning algorithm has been recently suggested by the Rainforth and Wood (2015). The main principle of the CCF is to create multiple DT classifier using the components estimated by the canonical correlation analysis ensuring the maximum correlation between the bands and the class labels (Colkesen and Kavzoglu, 2017; 2019).

3.3. Performance Evaluation

In this paper, as a standard process in image classification, classification results were evaluated using a standard error matrix to compute the overall accuracy and related statistics. Moreover, F-score measure was applied to conduct class-based performance evaluations. The F-score is the harmonic mean of precision (i.e. Producer's accuracy) and recall (i.e. User's accuracy) values. Furthermore, the McNemar's test was performed to test the statistical significance of the difference in accuracies between the classifiers. It is a non-parametric test based on χ^2 distribution was calculated to compare the classification errors of classifiers. If the calculated test statistic is greater than the χ^2 tabular value (i.e. 3.84 at 95% confidence interval), it is concluded that two classification results are statistically different.

4. RESULTS

In this study, OBIA with multi-resolution segmentation was performed to create image objects. It should be noted that the multi-resolution segmentation algorithm was performed in Definiens eCognition (9.1) software. The segmentation of WV-2 imagery was constructed by adjusting the user-defined scale, shape, compactness parameters and band weights. Based on a "trial and error" procedure, the multi-resolution segmentation parameters determined as 25-0.3-0.7 for scale, shape, compactness parameters, respectively. In addition, while all spectral band weights are set to 1, the two NIR bands were set to 2 due to its higher spectral effect on vegetation. At the end of the segmentation process, totally 308,460 image objects were created. In order to investigate the effects of the spectral indices of WV-2 image on the performance of object-based classification, 14 spectral indices given in Table 1 with their description, formulas and references were used.

Furthermore, the RF algorithm was also applied to estimate the relative importance of the 14 spectral vegetation indices for the classification process. The resulting feature subsets were presented in Figure 2. As can be seen from the figure, the most important vegetation indices were Chlorophyll RedEdge (3.28), green leaf indice (3.13) and NDVI-2 (2.68) indices, respectively. It should be noted that all indices were used in the classification process due to feature importance of all indices is greater than 0.5.

Table 1. Vegetation indices calculated from Worldview-2 data.

Indices	Formula	Source
NDVI-1	$\frac{\text{NIR1-Red}}{\text{NIR1+Red}}$	Tucker,1979
NDVI-2	$\frac{\text{NIR2-Red}}{\text{NIR2+Red}}$	Tucker,1979
Datt4	$\frac{\text{Re}d}{Green * \text{Re}dedge}$	Datt,1988
Chlorophyll Green	$(\frac{NIR}{Green})^{-1}$	Gitelson et al., 2006
Chlorophyll vegetation index	$NIR2 * \frac{\text{Re}d}{Green^2}$	Vincini et al., 2008
Enhanced Vegetation Index (EVI)	$2.5 * (\frac{NIR2 - \text{Re}d}{(NIR2 + 6 * \text{Re}d - 7.5 * Coastal) +$	Huete et al., 2002
Chlorophyll Index RedEdge	$\frac{NIR2}{\text{Re}d\ edge} - 1$	Gitelson et al., 2003
Green Leaf Index	$\frac{2 * Green - \text{Re}d - Coastal}{2 * Green + \text{Re}d + Coastal}$	Gobron et al., 2000
Green NDVI (GNDVI)	$\frac{\text{NIR2-Green}}{\text{NIR2+Green}}$	Gitelson et al., 1996
Green-Red NDVI	$\frac{\text{NIR2-(Green+Red)}}{\text{NIR2+(Green+Red)}}$	Wang et al., 2007
Modified NDVI	$\frac{NIR1 - \text{Re}d}{NIR1 + \text{Re}d - 2 * Coastal}$	Main et al., 2011
Red-Blue NDVI	$\frac{NIR2 - (\text{Re}d + Coastal)}{NIR2 + (\text{Re}d + Coastal)}$	Wang et al., 2007
Soil Adjusted Vegetation Index (SAVI)	$\frac{NIR1 - \text{Re}d}{NIR1 - \text{Re}d + 0.5} * (1.5)$	Huete, 1988
Spectral Polygon Vegetation Index (SPVI)	$0.4 * (3.7 * (NIR1 - \text{Re}d) - 1.2 * \lvert Green - \text{Re}d$	Main et al., 2011

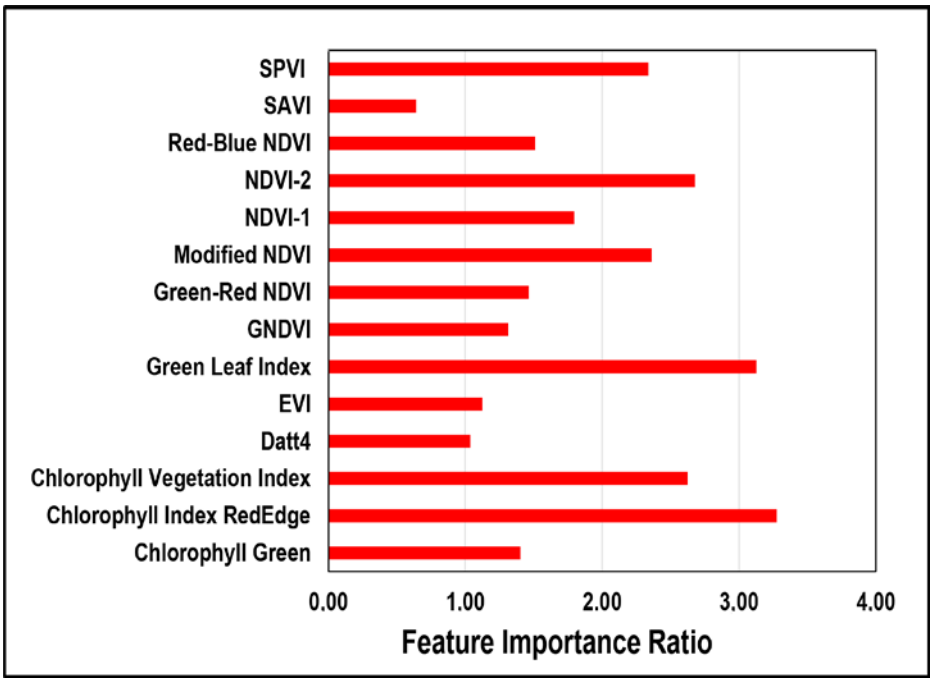

Figure 2. Vegetation Indices feature importance using RF feature selection algorithm

In addition, the mean values of each spectral band of image were calculated in the segmentation stage separately. In the classification stage, two combinations were performed using only mean values of the spectral bands (i.e., 8 subset) and using spectral bands and vegetation indices (i.e., 8+14=22 subset) together to compare the effect of vegetation indices on classification accuracy. Then, depending on the two spectral subset combinations, segmented images were classified using RF, CCF, DT, and k-NN classifiers. The accuracy results of all classifications with two subset combinations are summarized in Table 2.

Table 2. Classification accuracies summary for all combinations and methods

	8 subset F-score (%)				22 subset F-score (%)			
	CCF	RF	DT	KNN	CCF	RF	DT	KNN
Agriculture	89.40	87.72	82.30	87.29	88.58	85.96	82.30	86.31
Barren	95.13	89.78	86.09	90.99	96.60	92.22	86.09	90.72
Building	93.99	93.40	88.22	92.91	96.37	95.09	88.22	91.71
Concrete	95.29	94.22	93.62	92.64	94.92	92.68	93.62	92.86
Corn	98.83	96.89	94.94	98.06	98.72	98.39	94.94	98.49
Forest	90.77	84.61	81.11	83.74	91.32	87.05	81.11	85.50
Hazelnut	95.74	89.10	87.53	88.92	95.90	91.86	87.53	90.65
Road	93.28	91.91	89.83	90.60	93.78	91.38	89.83	90.99
Shadow	86.77	88.11	84.66	82.01	90.08	89.84	84.66	84.15
Soil	91.41	87.10	83.56	87.86	93.11	88.40	83.56	88.06
Water	95.65	92.12	85.83	89.80	93.28	95.32	85.83	96.94
OA (%)	93.89	90.36	87.41	89.81	94.55	91.95	87.56	90.87

As can be seen from the table that the highest overall accuracies were produced by CCF classifier with 93.89% and 94.55% for 8-subset and 22-subset combinations, respectively, whereas the lowest overall accuracies were computed by DT classifier with 87.41% and 87.56% for 8-subset and 22-subset combinations, respectively. Another important finding is that the CCF classifier helps to improve the classification performance up to 7% in overall accuracy compared to DT classifier. When the estimated F-score accuracies were analyzed, it was observed the highest accuracies were obtained for corn class by the CCF classifier with 98.83% and 98.72% for 8-subset and 22-subset combinations, respectively. In addition, it was observed that the use of spectral indices provides a positive contribution to overall accuracies for all classification methods.

To estimate the statistical significance of classification results, McNemar's test was performed between all classifiers for two subset combinations (Table 3). It should be noted that statistical tests were conducted at 95% confidence (i.e. 3.84) interval.

Table 3. McNemar's test results for comparing classifier performances

		RF	DT	KNN
8-Subset	CCF	52.28	122.30	59.25
	RF		29.61	0.93
	DT			15.26
		RF	DT	KNN
22-Subset	CCF	49.34	152.10	63.05
	RF		69.55	6.61
	DT			32.90

As can be seen from the table, all classification results were found to be a statistically significant except for the pairwise result of 8-subset RF and KNN classifier. Furthermore, thematic maps of the study area produced by the CCF classifier for both subset combinations were given in Figure 3. It should be noted that the CCF classification was chosen for thematic map producing because it gives the highest classification accuracy for both subset combinations. When the produced thematic maps were analyzed, it can be seen that both subset combinations produced similar results and assigned mainly same LULC classes. In particular, the 8-subset approach failed to distinguish mainly shadow areas compared to 22-subset approach.

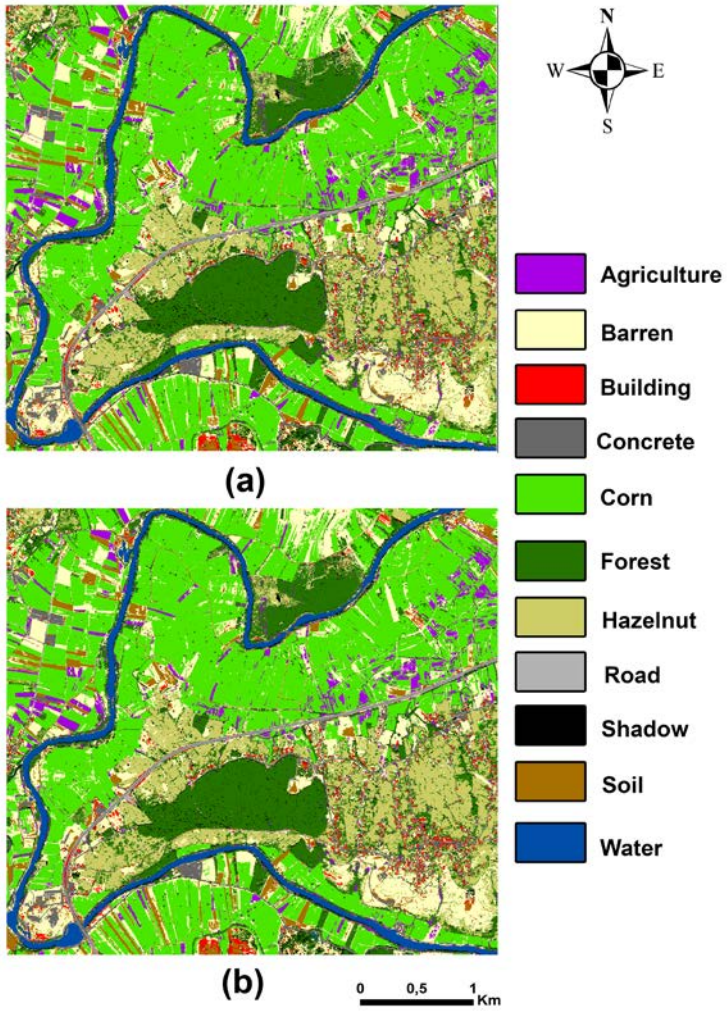

Figure 3. Thematic maps produced (a) 8-subset, (b) 22-subset using CCF classifier

5. CONCLUSION

The purpose of the current study was to map cultivated areas using four classification algorithms, namely RF, CCF, DT, k-NN classifiers in the classification of WV-2 imagery. In particular, various spectral indices have been used to identify and distinguish different cultivated areas and forest species. For this purpose, OBIA-based multi-resolution segmentation algorithm was employed for the segmentation process. The produced image objects were classified by using two subset combinations, namely 8-subset, 22-subset datasets. The results of this investigation showed that the CCF classifier performed the most accurate results for two subset combinations. Also the use of spectral vegetation indices contributed positively to overall classification accuracies for each classification algorithm. The results also indicated that approximately 7% classification accuracy improvement was achieved when the CCF classifier was applied to the image compared to DT classifier. Furthermore, McNemar's statistical test at 95% confidence interval confirmed that the difference in classification accuracy performance was statistically significant for all classification results except for between 8-subset RF and KNN classifier. Further studies are needed to determine the generality of the results of this study for different landscapes using various classification algorithms and spectral indices.

REFERENCE

Baatz, M., Schäpe A. 2000. Multiresolution Segmentation: an optimization approach for high quality multi-scale image segmentation. In: Strobl, Angewandte Geographische Informations- Verarbeitung XII, J., edited by Blaschke, T., Griesebner, Wichmann Verlag, Heidelberg, pp. 12-23.

Belgiu, M., Csillik, O., 2018. Sentinel-2 cropland mapping using pixel-based and object-based time-weighted dynamic time warping analysis. Remote Sensing of Environment, 204, pp. 509–523.

Breiman, L., 2001. Random Forests. Machine Learning, 45(1), pp. 5–32.

Cheng, H. D., Jiang, X. H., Sun, Y., Wang, J., 2001. Color image segmentation: advances and prospects. Pattern Recognition, 34(12), pp. 2259-2281.

Colkesen, I., Kavzoglu, T., 2017. Ensemble-based canonical correlation forest (CCF) for land use and land cover classification using Sentinel-2 and Landsat OLI imagery. Remote Sensing Letters, 8(11), pp.1082-1091.

Colkesen, I., Kavzoglu, T. 2019. Comparative evaluation of decision-forest algorithms in object-based land use and land cover mapping. In: Spatial modeling in GIS and R for earth and environmental science, edited by H. R. Pourghasemi and C. Gokceoglu, Elsevier. pp. 499-517.

Datt, B., 1998. Remote sensing of chlorophyll a, chlorophyll b, chlorophyll a + b, and total carotenoid content in Eucalyptus leaves. Remote Sensing of Environment, 66, pp. 111-121.

Ghebreamlak, A.Z., Tanakamaru, H., Tada, A., Adam, B.M.A., Elamin, K.A.E., 2018. Satellite-based mapping of cultivated area in Gash Delta Spate Irrigation System, Sudan. Remote Sensing, 10, pp. 2.

Gitelson, A. A., Kaufman, Y. J., Merzlyak, M. N., 1996, Use of a green channel in remote sensing of global vegetation from EOS-MODIS. Remote Sensing of Environment, 58, pp. 289-298.

Gitelson, A. A., Viña, A., Arkebauer, T. J., Rundquist, D. C., Keydan, G., Leavitt, B., 2003. Remote estimation of leaf area index and green leaf biomass in maize canopies. Geophysical Research Letters, 30, pp. 1248.

Gitelson, A. A., Keydan, G. P., Merzlyak, M. N., 2006, Three-band model for noninvasive estimation of chlorophyll, carotenoids, and anthocyanin contents in higher plant leaves. Geophysical Research Letters, 33, pp. L11402.

Gobron, N., Pinty, B., Verstraete, M. M., Widlowski, J. L., 2000. Advanced vegetation indices optimized for up-coming sensors: Design, performance, and applications. IEEE Transactions on Geoscience and Remote Sensing, 38, pp. 2489-2505.

Huete, A. R., 1988, A Soil-Adjusted Vegetation Index (SAVI). Remote Sensing of Environment, 25, pp. 295- 309.

Huete, A., Didan, K., Miura, T., Rodriguez, E. P., Gao, X., Ferreira, L. G., 2002. Overview of the radiometric and biophysical performance of the MODIS vegetation indices. Remote Sensing of Environment, 83, pp.195-213.

Hughes, G. F. 1968. On the mean accuracy of statistical pattern recognizers. IEEE Transactions on Information Theory, 14(1), pp. 55-63.

Immitzer, M., Atzberger, C., Koukal, T., 2012. Tree species classification with random forest using very high spatial resolution 8-band Worldview-2 satellite data. Remote Sensing, 4, pp. 2661–2693.

Inglada, J., Arias, M., Tardy, B., Hagolle, O., Valero, S., Morin, D., Koetz, B., 2015. Assessment of an operational system for crop type map production using high temporal and spatial resolution satellite optical imagery. Remote Sensing, 7(9), pp. 12356–12379.

Kavzoglu, T., Mather, P. M., 2000. The use of feature selection techniques in the context of artificial neural networks. In Proceedings of the 26th annual conference of the remote sensing society, Leicester, UK. September 12–14.

Kavzoglu, T., Colkesen, I., 2013. An assessment of effectiveness of rotation forest ensemble for land use and land cover mapping. International Journal of Remote Sensing, 34(12), pp. 4224-4241.

Kavzoglu, T. Yildiz Erdemir, M., Tonbul, H., 2016. A region-based multi-scale approach for object-based image analysis. In: International Society for Photogrammetry and Remote Sensing (ISPRS) 2016-XXIII Congress, 9-12 July 2016, Prague-Czech Republic, XLI-B7, pp. 241-247.

Kavzoglu,T. Yildiz Erdemir, M., Tonbul, H., 2017, Classification of semiurban landscapes from very high-resolution satellite images using a regionalized multiscale segmentation approach. Journal of Applied Remote Sensing, 11(3), pp. 035016.

Kavzoglu, T., Tonbul, H., 2018. An experimental comparison of multi-resolution segmentation, SLIC and K-Means clustering for object-based classification of VHR imagery. International Journal of Remote Sensing, 39(18), pp.6020-6036.

Kavzoglu, T., Tonbul, H., Yildiz Erdemir, M., Colkesen, I., 2018, Dimensionality reduction and classification of hyperspectral ımages using object-based ımage analysis, Journal of the Indian Society of Remote Sensing, 46(8), pp. 1297-1306.

Kenduiywo, B.K., Bargiel, D., Soergel, U., 2018. Crop-type mapping from a sequence of Sentinel-1 images. International Journal of Remote Sensing, 39, pp. 6383–6404.

Liu, Y., Bian, L., Meng, Y., Wang, H., Zhang, S., Yang, Y., Shao, X., Wang, B., 2012. Discrepancy measures for selecting optimal combination of parameter values in object-based image analysis. ISPRS Journal of Photogrammetry and Remote Sensing, 68, pp. 144–156.

Main, R., Cho, M.A., Mathieu, R., O'Kennedy, M.M., Ramoelo, A., Koch, S., 2011. An investigation into robust spectral indices for leaf chlorophyll estimation. ISPRS Journal of Photogrammetry and Remote Sensing 66(6), pp.751–761.

Mokhtari, A., Noory, H., Pourshakouri, F., Haghighatmehr, P., Afrasiabian, Y., Razavi, M., Fereydooni, F., Naeni, A.S., 2019. Calculating potential evapotranspiration and single crop coefficient based on energy balance equation using Landsat 8 and Sentinel-2. ISPRS Journal of Photogrammetry and Remote Sensing, 154, pp. 231–245.

Mui, A., He, Y., Weng, Q., 2015. An object-based approach to delineate wetlands across landscapes of varied disturbance with high spatial resolution satellite imagery. ISPRS Journal of Photogrammetry and Remote Sensing ,109, pp. 30–46.

Numbisi, F.N., Van Coillie, F.M.B., De Wulf, R., 2019. Delineation of cocoa agroforests using multiseason Sentinel-1 SAR images: a low grey level range reduces uncertainties in GLCM texture-based mapping. ISPRS International Journal of Geo-Information, 8(4), pp. 179.

Rainforth, T., Wood, F., 2015. Canonical correlation forests. [accessed 2019 August 9]. https://arxiv.org/pdf/1507.05444.pdf.

Sonobe, R., Yamaya, Y., Tani, H., Wang, X., Kobayashi, N., Mochizuki, K.-I., 2018. Crop classification from Sentinel-2-derived vegetation indices using ensemble learning. Journal of Applied Remote Sensing, 12, pp. 026019.

Tucker, C. J., 1979. Red and photographic infra-red linear combinations for monitoring vegetation, Remote Sensing of Environment, 8(2), pp. 127–150.

Vincini, M., Frazzi, E., D'Alessio, P., 2008, A broad-band leaf chlorophyll vegetation index at the canopy scale. Precision Agriculture, 9, pp. 303–319.

Wang, F., Huang, J., Tang, Y., Wang, X., 2007. New vegetation index and its application in estimating leaf area index of rice, Rice Science, 14(3), pp.195−203.